Near infrared oximetry-guided artery–vein classification in optical coherence tomography angiography

Taeyoon Son[1], Minhaj Alam[1], Tae-Hoon Kim[1], Changgeng Liu[1], Devrim Toslak[1,2] and Xincheng Yao[1,3]

[1]Department of Bioengineering, University of Illinois at Chicago, Chicago, IL 60607, USA; [2]Department of Ophthalmology, Antalya Training and Research Hospital, Antalya 07100, Turkey; [3]Department of Ophthalmology and Visual Sciences, University of Illinois at Chicago, Chicago, IL 60612, USA

Corresponding author: Xincheng Yao. Email: xcy@uic.edu

Impact statement

It is known that arteries and veins can be affected by retinal diseases differently. Therefore, quantitative artery–vein analysis holds the promise for better disease detection and treatment evaluation. However, clinical optical coherence tomography (OCT) and optical coherence tomography angiography (OCTA) instruments lack the function of differential artery–vein analysis. Here, we report the feasibility of near infrared OCT oximetry-guided artery–vein classification in OCTA. Because the OCT and OCTA are naturally captured from the same instrument simultaneously, the presented method is feasible for practical deployment of differential artery–vein analysis in OCTA.

Abstract

Differential artery–vein analysis is valuable for early detection of diabetic retinopathy and other eye diseases. As a new optical coherence tomography imaging modality, optical coherence tomography angiography provides capillary level resolution for accurate examination of retinal vasculatures. However, differential artery–vein analysis in optical coherence tomography angiography particularly for macular region in which blood vessels are small is challenging. In coordination with an automatic vessel tracking algorithm, we report here the feasibility of using near infrared optical coherence tomography oximetry to guide artery–vein classification in optical coherence tomography angiography of macular region.

Keywords: Optical coherence tomography, optical coherence tomography angiography, artery and vein classification, retina, ophthalmology

***Experimental Biology and Medicine* 2019; 244: 813–818. DOI: 10.1177/1535370219850791**

Introduction

It is known that pathological alterations in the artery and vein can be affected in different ways.[1] For example, diabetic retinopathy (DR) and retinopathy of prematurity (ROP) may result in increased arterial tortuosity, venous beading, narrowing artery, and dilated vein.[2] Therefore, quantitative analysis of arteries and veins is essential for better disease diagnosis and treatment evaluation. Artery–vein classification of blood vessels in color fundus images has been demonstrated.[3,4] However, traditional fundus photography only works for major vessel branches due to the image resolution and contrast limits. Because many of systemic diseases are related to microvascular abnormalities,[5–9] it is important to classify the arteries and veins in retinal microvascular networks, particularly for the macular region.

Optical coherence tomography angiography (OCTA) provides a noninvasive, three-dimensional imaging modality capable of providing high-resolution observation of the microvascular networks at capillary level.[10] Multiple OCTA features, such as blood vessel caliber (BVC), blood vessel tortuosity (BVT), vessel perimeter index, foveal avascular zone (FAZ) area, FAZ contour irregularity, and retinal vascular density, have been developed for quantitative OCTA analysis and computer-aided classification of age-related Macular Degeneration,[11] DR,[12] glaucoma,[13] and sickle cell

retinopathy.[10] Recently, we demonstrated the feasibility of using color fundus image to guide artery–vein differentiation in OCTA.[14] Two differential artery–vein features, i.e. artery vein ratio of blood vessel caliber (AVR-BVC) and tortuosity (AVR-BVT) improved the performance of DR classification. However, clinical deployment of the color fundus image-guided OCTA analysis requires the involvements of two clinical instruments, i.e. fundus camera and OCTA system, and sophisticated image registration. In this study, we demonstrated the feasibility of using only optical coherence tomography (OCT) information to conduct artery–vein classification. In coordination with automatic vessels tracking algorithm,[15] near infrared (NIR) OCT oximetry analysis was demonstrated to achieve reliable guidance of the artery–vein classification in OCTA.

Methods and materials

Subjects

This study was approved by the Institutional Review Board of the University of Illinois at Chicago and followed the tenets of the Declaration of Helsinki. Eight normal subjects (eight men, mean age 29.63 ± 6.46 years) were recruited from the Lions of Illinois Eye Research Institute of the University of Illinois. All subjects were healthy individuals without history of ocular disease. Informed consent was provided by each subject before participation in the study.

Experimental setup

Figure 1(a) illustrates a schematic diagram of the custom-designed OCT/OCTA used for this study. An NIR superluminescent diode (SLD; D-810-HP, Superlum, Cork, Ireland), which has a center wavelength of 810 nm (bandwidth: 760–860 nm), was selected for this study. Since the NIR SLD covers 760–860 nm (Figure 1(b1)), it allows easy comparison between our proposed 765/805 nm optical density ratio (ODR) analysis and previous 805/855 nm ODR analysis. A fiber coupler with a splitting ratio of 90:10 divided the SLD light into the sample and reference arms. In the sample arm, the light was delivered to the eye through relay optical lenses. One pair of scanning mirrors was used to produce two-dimensional scanning over the retina for OCT acquisition. A 70,000 Hz line-scan CCD camera with 2048 pixels was used in the OCT spectrometer. The axial and lateral resolutions were estimated at 3 μm and 12 μm, respectively. A pupil camera was used to aid retinal localization, and a fixation target with dim green light was used to minimize voluntary eye movements. For OCT recording, the illumination power on the cornea was set at ~600 μW. Four B-scan OCTs were acquired from macular region, and speckle variance processing was used for OCTA image construction.

Image acquisition

One eye of each volunteer was used for OCT recording. During the alignment for retinal imaging, the subject was instructed to follow a fixation target, while the operator

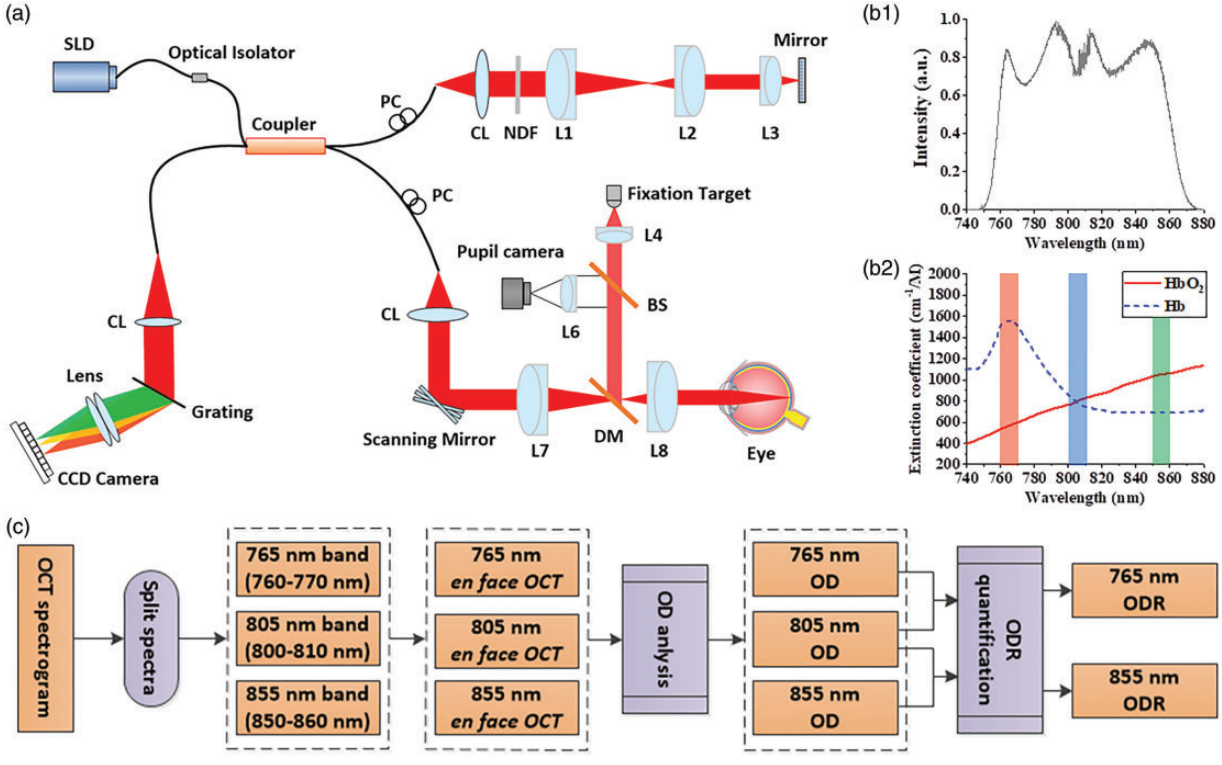

Figure 1. (a) Schematic diagram of the OCT system. (b1) Spectral intensity of the NIR SLD light source. (b2) Absorption spectra of oxyhemoglobin (HbO_2) and deoxyhemoglobin (Hb). The red, green, and blue rectangles indicate oxygen-sensitive 765 nm, oxygen-sensitive 855 nm, and oxygen-isosbestic 805 nm light windows used for ODR analysis. (c) Flow chart of ODR analysis at different spectral bands. CL: collimation lens; DM: dichroic mirror; Lenses: L1, L2, L3, L4, L5, L6, L7, L8; NDF: neutral density filter; PC: polarization controller; SLD: superluminescent diode; DM: dichroic mirror; BS: beam splitter. (A color version of this figure is available in the online journal.)

monitored the real-time OCT scans and pupil camera to locate a region-of-interest (ROI). Once we identified the desired ROI, we asked the subject to keep his eyes wide open and refrain from blinking during the image acquisition.

Artery–vein classification

We have recently combined color fundus oximetry analysis and blood vessel tracking to guide the artery–vein classification in OCTA.[14] Here, the *en face* OCT will function as a color fundus image to conduct optical density (OD) analysis. The OD, i.e. the light absorbance of each blood vessel, relative to surrounding tissue, can be estimated as $\ln(I_{\lambda 0}/I_{\lambda})$, where I_{λ} and $I_{\lambda 0}$ are the average intensity values of the blood vessel and avascular background area with illumination light wavelength λ. It is known that the oxyhemoglobin (HbO_2) and deoxyhemoglobin (Hb) absorptions are sensitive to the wavelength (Figure 1(b2)). ODR between those measured at oxygen sensitive wavelengths and isosbestic wavelengths is linearly proportional to blood oxygen saturation.[16,17] The ODR can be used for artery–vein classification and can be calculated as

$$\mathrm{ODR}_{\lambda} = \frac{\mathrm{OD}_{\mathrm{sensitive}}}{\mathrm{OD}_{\mathrm{isosbestic}}}$$

where $\mathrm{OD}_{\mathrm{sensitive}}$ and $\mathrm{OD}_{\mathrm{isosbestic}}$ are optical densities at oxygen-sensitive (765 nm) and oxygen-isosbestic wavelengths (805 nm), respectively (Figure 1(b2)). In order to optimize the sensitivity of ODR analysis required for artery–vein classification, the 765 nm was specially selected as oxygen-sensitive wavelength. The oxygen-sensitive wavelength for OCT oximetry analysis was 855 nm,[16,17] with limited signal-to-noise ratio. As shown in Figure 1 (b2), the extinction coefficient difference between HbO_2 and Hb around 765 nm is 2.76 times higher than 855 nm used in previous studies.[16,17] For comparative assessment, we quantified the ODRs for both 765 nm/805 nm and 855 nm/805 nm combinations. Figure 1(c) illustrates the core steps of the ODR analysis at different spectral bands.

In order to ensure reliable artery–vein classification, we conducted the ODR analysis at the optic disc region in *en face* OCT, and blood vessel tracing was used to track the arteries and veins into the macular region.[14]

Results

Figure 2(a) illustrates representative B-scan OCT (Figure 2 (a1)), *en face* OCT (Figure 2(a2)) and OCTA (Figure 2(a3)) images of macular region. The B-scan OCT image clearly revealed individual layers in the retina, including the nerve fiber layer, ganglion cell layer, inner plexiform layer, inner nuclear layer, outer plexiform layer, outer nuclear layer, external limiting membrane, inner segment/outer segment, and retinal pigment epithelium and choroid (Figure 2(a1)). The *en face* OCT image enabled fundus visualization of the macula (fovea) and retinal blood vessels (Figure 2(a2)). In comparison with the *en face* OCT image (Figure 2(a2)), the OCTA image increased the visibility of blood vessels with capillary level resolution (Figure 2(a3)). The *en face* OCT and OCTA consist of 350×350 pixels, corresponding to a 3.5 mm $\times$ 3.5 mm retinal area.

Direct artery–vein classification of small blood vessels around the macular region is difficult due to the small dimension and limited contrast compared to background intensity (Figure 2(a2)). In order to overcome this problem, we collected nine OCT volumes to produce retinal OCT fundus image to cover both the optic disc and macular regions (Figure 2(b)). The blood vessels within the optic disc region (Figure 2(c1)) have relatively large diameter, and thus can be readily used for artery–vein classification. Ten sampling locations were selected from the edge and surrounding tissue for normalized ODR analysis (Figure 2(c2)). The edges of the blood vessels were chosen to reduce the influence of central reflex (Figure 2(c3)). Figure 2(d1) and Figure 2(d2) show ODRs of individual blood vessels in Figure 2(c1) using 765 nm and 855 nm as oxygen-sensitive wavelengths, respectively. Arteries consistently revealed smaller ODRs compared to that of the veins at 765 nm wavelength (Figure 2(d1)) and larger ODRs in arteries compared to that of the veins at 855 nm wavelength (Figure 2(d2)). ODRs from all eight subjects consistently confirmed the observation (Figure 2(e1) and (e2)). The averaged ODR of all vessel nodes can work as a practical thresholding criterion to separate arteries and veins readily for 765/805 nm analysis (Figure 2(e1)), while the averaged ODR cannot be used to reliably separate arties and veins for 805/855 nm analysis (Figure 2(e2)). The ODR difference between artery and vein was calculated to validate ODR sensitivity (Figure 2(f)). The ODR difference showed 2.29 times higher at 765 nm oxygen-sensitive wavelength (0.48 ± 0.03; mean $\pm$ standard error) than 855 nm oxygen-sensitive wavelength (0.21 ± 0.02; mean $\pm$ standard error).

Figure 3(a) shows segmented vessel map corresponding to the *en face* OCT in Figure 2(b), by implementing global thresholding method, and optic disc is identified based on gradient intensity information. The source nodes are detected around the optic disc to make a start point for each vessel tracking and identified as red and blue for artery and vein, respectively, based on the ODR analysis explained in Figure 2. A skeletonized vessel map for the vessel tracking is shown in Figure 3(b). The blood vessel tracking algorithm started at a nodal point and tracked the branch until it reached the end point within macular region. The procedure was completed till all branches were classified into arteries or veins. OCT artery–vein map was generated by inverse distance transform (Figure 3(c)).

Because the OCTA image was reconstructed based on speckle variance analysis of the OCT, the OCTA image is naturally registered with the OCT image (Figure 3(d)). Therefore, the OCT artery–vein map (Figure 3(c)) can be used to guide the artery–vein classification in the OCTA image (Figure 3(d)). Upon registration, the OCT artery–vein map was mapped into the OCTA image. The blood vessel branches in the OCTA image were connected with the branches in OCT artery–vein map. They were further tracked from branches of OCT artery–vein map to the end of OCTA branches accordingly. The tracking algorithm and

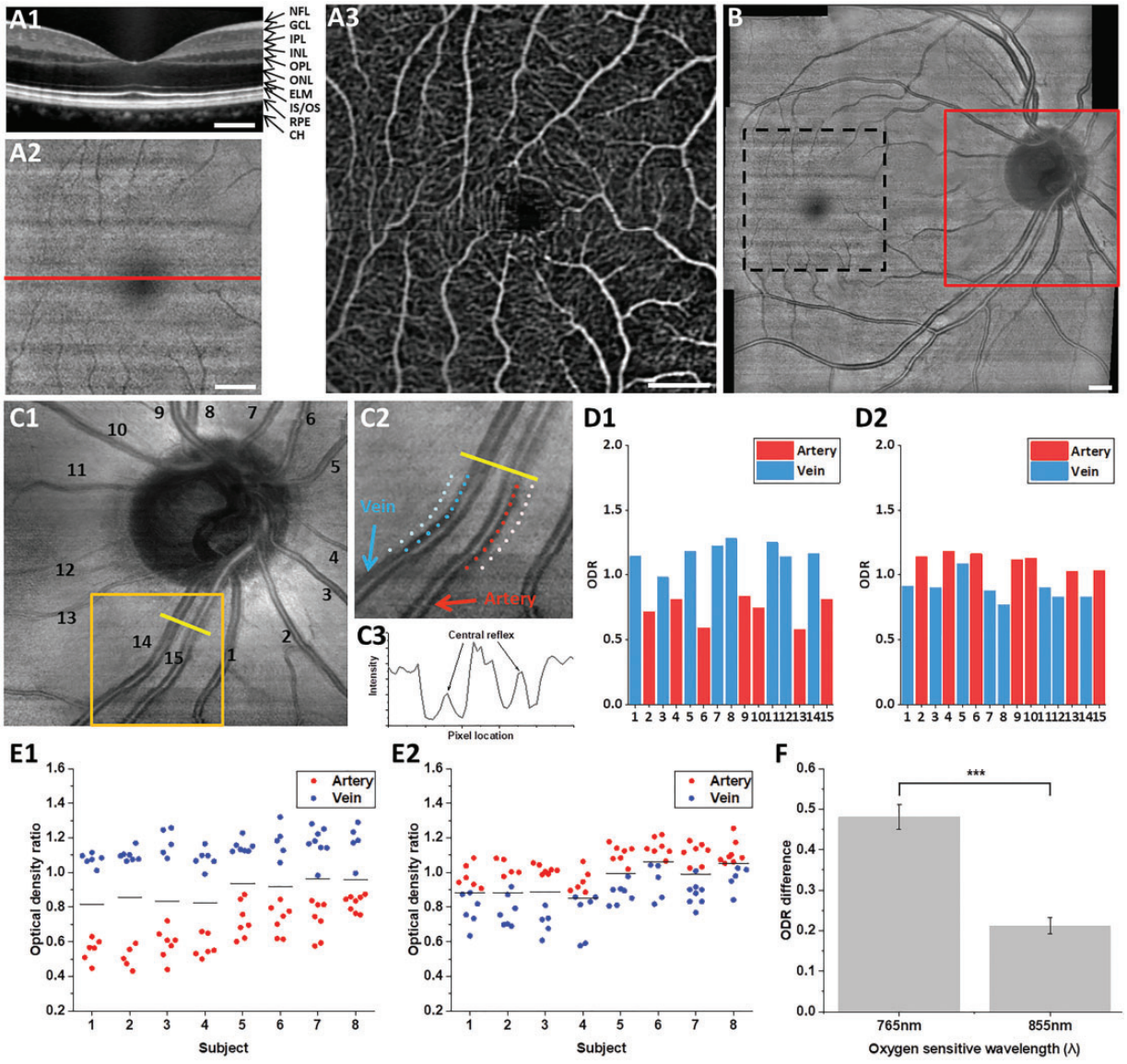

Figure 2. Representative B-scan OCT (a1), *en face* OCT (a2), and OCTA (a3) images from the macula. The horizontal line in (a2) indicates the location of B-scan OCT in (a1). (b) OCT fundus covering optic disc and macular regions. *En face* OCT from optic disc (c1), sampling locations of vessels and tissue area (c2), intensity profile over vessels and tissue (c3). ODRs from vessels in (c1) at 765 nm (d1) and 855 nm (d2). ODRs from each subject with 765/805 nm analysis (e1) and 805/855 nm analysis (e2). Solid black lines indicate averaged ODR of all artery and vein ODRs for each subject. (f) Averaged ODR difference of artery and vein from different oxygen-sensitive wavelength. Scale bars: 500 μm. (A color version of this figure is available in the online journal.)

artery–vein classification followed the same protocol used for OCT artery–vein map. Figure 3(e) shows the OCTA artery–vein map guided by OCT artery–vein map. The arteries and veins in macular region were fully classified, showing more capillary details compared to the OCT artery–vein map of the same macular region (Figure 3(f)).

Discussion

In summary, we demonstrated the feasibility of using NIR light oximetry analysis in OCT to guide the artery–vein classification in OCTA. 765 nm/805 nm ODR analysis provided a robust artery–vein difference in NIR OCT to provide reliable guidance required for artery–vein classification in OCTA. Visible light OCT[18] has been established for retinal oximetry measurements.[19,20] However, the visible light may lead to retinal stimulation.[19,20] NIR light (855 nm used as an oxygen-sensitive wavelength) has also been explored for retinal oximetry, but low signal-to-noise ratio limited its practical application for clinical deployment.[16,17] In order to optimize the ODR sensitivity, we selected an NIR source with a center wavelength at 810 nm, which is shorter compared to that (typically > 840 nm) used in commercial OCTs. Using the 810-nm SLD, we were able to differentiate arteries and veins reliably. ODR of 805 nm/855 nm combination is consistent with previously reported findings from Kagemann et al.[17] and Ye et al.,[16] while ODR of 765 nm/805 nm significantly improved the robustness of NIR oximetry for reliable artery–vein differentiation in OCTA. It is well established that eye diseases, such as DR and ROP, often affect the diameter and tortuosity of arteries and veins in different

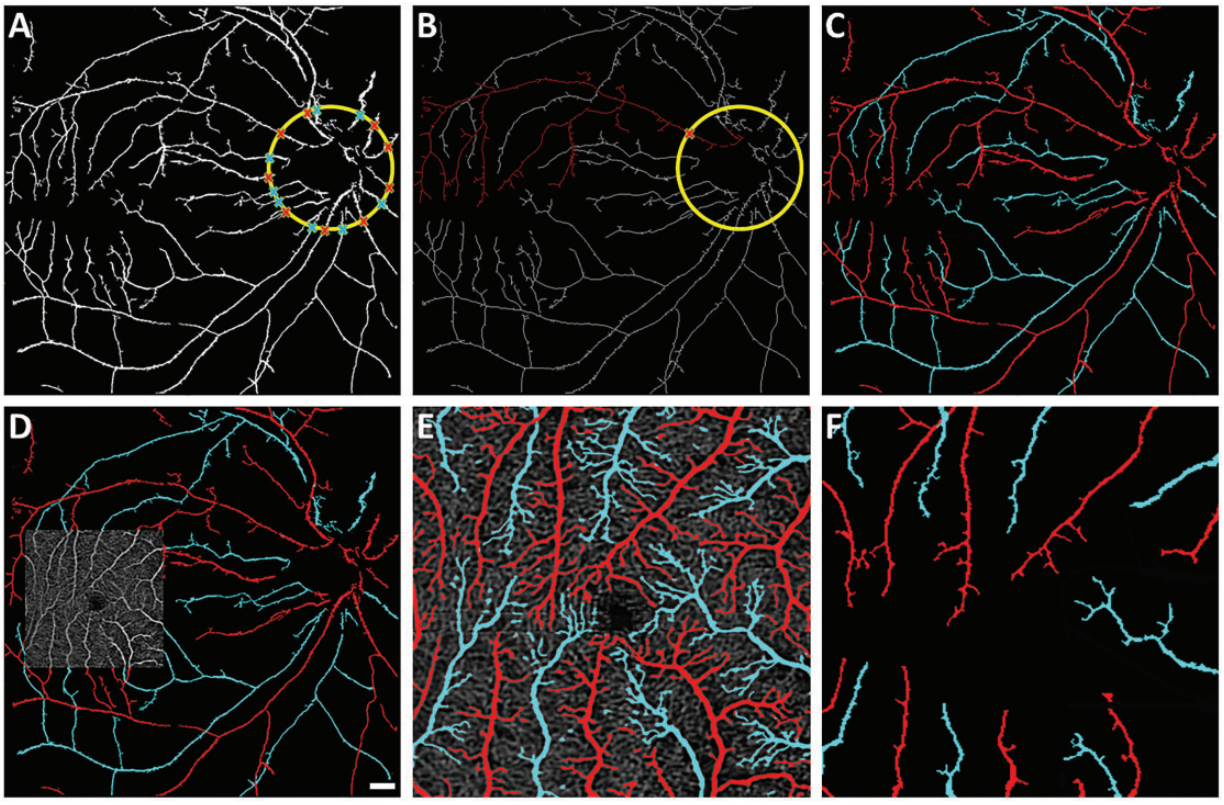

Figure 3. (a) Segmented vessel map from the *en face* OCT shown in Figure 2(b). Source nodes are marked for artery/vein classification. (b) Skeletonized OCT vessel map showing representative blood vessel tracking from the source node. (c) OCT artery–vein map. (d) OCTA is registered to the macular region of OCT artery–vein map in C. (e) Macular OCTA artery–vein map. (f) Macular OCT artery–vein map. (A color version of this figure is available in the online journal.)

way. We anticipate that differential artery–vein analysis will improve the sensitivity of quantitative OCTA detection and classification of eye diseases.

Authors' contributions: TS performed data acquisition, data analysis, and manuscript preparation; MA and TK contributed to data analysis; CL contributed to data acquisition; DT contributed to data analysis; XY supervised the study and contributed to data analysis and manuscript preparation.

DECLARATION OF CONFLICTING INTERESTS

The author(s) declared no potential conflicts of interest with respect to the research, authorship, and/or publication of this article.

FUNDING

The author(s) disclosed receipt of the following financial support for the research, authorship, and/or publication of this article: This research was supported in part by NIH grants R01 EY023522, R01 EY030101, P30 EY001792; by Richard and Loan Hill endowment; by unrestricted grant from Research to Prevent Blindness.

ORCID iD

Taeyoon Son https://orcid.org/0000-0001-7273-5880
Tae-Hoon Kim https://orcid.org/0000-0002-4391-4860

REFERENCES

1. Ouyang Y, Shao Q, Scharf D, Joussen AM, Heussen FM. An easy method to differentiate retinal arteries from veins by spectral domain optical coherence tomography: retrospective, observational case series. *BMC Ophthalmol* 2014;**14**:66
2. Joshi VS, Reinhardt JM, Garvin MK, Abramoff MD. Automated method for identification and artery-venous classification of vessel trees in retinal vessel networks. *PLoS One* 2014;**9**:e88061
3. Huang F, Dashtbozorg B, Romeny BM. Artery/vein classification using reflection features in retina fundus images. *Mach Vision Appl* 2018;**29**:23–34
4. Miri M, Amini Z, Rabbani H, Kafieh R. A comprehensive study of retinal vessel classification methods in fundus images. *J Med Signals Sens* 2017;**7**:59–70
5. Cabrera DeBuc D, Somfai GM, Koller A. Retinal microvascular network alterations: potential biomarkers of cerebrovascular and neural diseases. *Am J Physiol Heart Circ Physiol* 2017;**312**:H201–12
6. Newman A, Andrew N, Casson R. Review of the association between retinal microvascular characteristics and eye disease. *Clin Exp Ophthalmol* 2017;**46**:531–552
7. Rani A, Mittal DD. Measurement of arterio-venous ratio for detection of hypertensive retinopathy through digital color fundus images. *J Biomed Eng Med Imaging* 2015;**2**:35–45
8. Heitmar R, Nicholl P, Lee B, Lau YC, Lip G. The relationship of systemic markers of haemostasis with retinal blood vessel responses in cardiovascular disease and/or diabetes. *Br J Biomed Sci* 2018;**75**:1–6
9. Patton N, Aslam T, Macgillivray T, Pattie A, Deary IJ, Dhillon B. Retinal vascular image analysis as a potential screening tool for cerebrovascular disease: a rationale based on homology between cerebral and retinal microvasculatures. *J Anat* 2005;**206**:319–48
10. Alam M, Thapa D, Lim JI, Cao D, Yao X. Quantitative characteristics of sickle cell retinopathy in optical coherence tomography angiography. *Biomed Opt Express* 2017;**8**:1741–53

11. Palejwala NV, Jia Y, Gao SS, Liu L, Flaxel CJ, Hwang TS, Lauer AK, Wilson DJ, Huang D, Bailey ST. Detection of nonexudative choroidal neovascularization in age-related macular degeneration with optical coherence tomography angiography. *Retina* 2015;**35**:2204–11
12. Kim AY, Chu Z, Shahidzadeh A, Wang RK, Puliafito CA, Kashani AH. Quantifying microvascular density and morphology in diabetic retinopathy using spectral-domain optical coherence tomography angiography. *Invest Ophthalmol Vis Sci* 2016;**57**:362–70
13. Hollo G. Vessel density calculated from OCT angiography in 3 peripapillary sectors in normal, ocular hypertensive, and glaucoma eyes. *Eur J Ophthalmol* 2016;**26**:e42–5
14. Alam M, Toslak D, Lim JI, Yao XC. Color fundus image guided artery-vein differentiation in optical coherence tomography angiography. *Invest Ophthalmol Vis Sci* 2018;5:4953-4962
15. Alam M, Son T, Toslak D, Lim JI, Yao X. Combining ODR and blood vessel tracking for artery-vein classification and analysis in color fundus images. *Transl Vis Sci Technol* 2018;**7**:23
16. Ye Y, Jiang H, Shen M, Lam BL, Debuc DC, Ge L, Sehi M, Wang J. Retinal oximetry using ultrahigh-resolution optical coherence tomography. *Clin Ophthalmol* 2012;**6**:2085–92
17. Kagemann L, Wollstein G, Wojtkowski M, Ishikawa H, Townsend KA, Gabriele ML, Srinivasan VJ, Fujimoto JG, Schuman JS. Spectral oximetry assessed with high-speed ultra-high-resolution optical coherence tomography. *J Biomed Opt* 2007;**12**:041212
18. Zhang X, Hu J, Knighton RW, Huang XR, Puliafito CA, Jiao S. Dual-band spectral-domain optical coherence tomography for in vivo imaging the spectral contrasts of the retinal nerve fiber layer. *Opt Express* 2011;**19**:19653–9
19. Chen S, Shu X, Nesper PL, Liu W, Fawzi AA, Zhang HF. Retinal oximetry in humans using visible-light optical coherence tomography (Invited). *Biomed Opt Express* 2017;**8**:1415–29
20. Pi S, Camino A, Cepurna W, Wei X, Zhang M, Huang D, Morrison J, Jia Y. Automated spectroscopic retinal oximetry with visible-light optical coherence tomography. *Biomed Opt Express* 2018;**9**:2056–67

(Received February 18, 2019, Accepted April 19, 2019)